Photonic Sensors (2011) Vol. 1, No. 3: 260–267

DOI: 10.1007/s13320-010-0009-9 **Photonic Sensors**

Regular

Loop Topology Based White Light Interferometric Fiber Optic Sensor Network for Application of Perimeter Security

Libo YUAN[1] and Yongtao DONG[2]

[1]*Key Laboratory of Optical Fiber Sensors (Heilongjiang Province), Photonics Research Center, College of Science, Harbin Engineering University, Harbin, 150001, China*

[2]*Department of Civil and Environmental Engineering, University of Alaksa Fairbanks, Fairbanks, AK 99709, USA*

* Corresponding author: Libo YUAN E-mail: lbyuan@vip.sina.com

Abstract: A loop topology based white light interferometric sensor network for perimeter security has been designed and demonstrated. In the perimeter security sensing system, where fiber sensors are packaged in the suspended cable or buried cable, a bi-directional optical path interrogator is built by using Michelson or Mach-Zehnder interferometer. A practical implementation of this technique is presented by using an amplified spontaneous emission (ASE) light source and standard single mode fiber, which are common in communication industry. The sensor loop topology is completely passive and absolute length measurements can be obtained for each sensing fiber segment so that it can be used to measure quasi-distribution strain perturbation. For the long distance perimeter monitoring, this technique not only extends the multiplexing potential, but also provides a redundancy for the sensing system. One breakdown point is allowed in the sensor loop because the sensing system will still work even if the embedded sensor loop breaks somewhere.

Keywords: Optical fiber sensors, quasi-distributed sensing system, perimeter security, white light interferometry

1. Introduction

Fiber optic sensing systems have been used in security applications for many years. It started from simple system where only an alarm was generated when a fiber was cut or broken. Now, there is a growing interest in research to detect and locate the disturbance using fiber optic sensors. This could be especially useful for perimeter security. In comparison with other sensors, fiber optic sensors are passive and sensitive to a variety of parameters. Long-gauge distributed or quasi-distributed fiber optic sensing system can be used for intruder localization. First demonstration of the possibility of locating the disturbed phase using distributed sensors based on a combination of Sagnac and Mach-Zehnder interferometers was published by Dakin *et al*. [1] in 1987. Spammer *et al*. also described the inteferometric technique to detect and locate perturbations by merging a Sagnac interferometer with a Michelson interferometer [2]. In 2001, Szustakowski developed a fiber distributed sensor based on a combination of Sagnac and Sagnac interferometers [3]. Culshaw *et al*. proposed a fiber distributed sensing system based on an internal modal interference technology in 2000 [4]. Thereafter, the distributed vibration fiber optic sensor was also developed by using Mach-Zehnder interferometer [5, 6]. The other examples of such sensing systems are fiber Bragg grating sensors [7, 8], optical time domain reflectometry (OTDR), and Brillouin optical time domain reflectometry

Received: 17 September 2010 / Revised version: 8 October 2010

(BOTDR) distributed sensors [9, 10]. White light interferometry, as a technique employing low coherence broadband light sources, is also one of attractive and potential candidate for application of perimeter security. The idea of using a short coherence length source to separate the signals returning from a series of sensors was first published by Al-Chalabi *et al.* [11]. Brooks *et al*. proposed a series of Mach-Zehnder interferometers and ladder coherence multiplexing schemes [12]. Valeria Gusmeroli reported a low coherence polarimetric sensor array multiplexed on fiber lines [13]. Sorin *et al*. [14] and Inaudi *et al*. [15] further developed and simplified the quasi-distributed low coherence fiber optic sensor array based on Michelson interferometer. In comparison with the several distributed fiber sensing systems mentioned above, white light fiber optic interferometric quasi-distributed sensors are simple and low in cost, and have flexibility of the gauge length, and therefore they are attractive for the application in perimeter security.

In this paper, a white light interferometric fiber optic sensor loop network has been designed for distributed perimeter monitoring. The system uses a scanning Mach-Zehnder interferometer or Michelson interferometer to interrogate the changes of optical path of fiber optic sensors from bi-direction of the optical fiber loop. The system is capable of making absolute measurements of high resolution. The parameters that can be measured include strain or other perturbations. White light interferometers can be configured to perform quasi-distributed measurement by multiplexing a number of sensors on the fiber loop. This is advantageous since it not only extends the multiplexing capacity, but also provides a redundancy and improves the reliability of the sensing system in case of potential damage to the buried sensor chain. Therefore, the loop topology based sensor network not only satisfies the redundancy requirement for a practical sensing system, but also provides a damage diagnosis methodology for large-scale perimeter security monitoring system.

2. Bi-directional interrogation technique (BDIT) based on a loop topology

Similar to other coherence-multiplexed schemes, BDIT uses separate receiving interferometers whose time delays are matched to the remote sensing gauge reflective signal pair. It is classified into two types based on Mach-Zehnder and Michelson interrogation architecture [16, 17] as shown in Figs. 1 and 2. The common characteristic of these schemes is that the sensors are connected and linked one by one to form a fiber loop topology, which ensure that it can be interrogated in both directions. In this sense, one of the advantages of BDIT is the enhanced multiplexing capacity. It can double the number of sensors when being compared to the single end array system. The looped sensors are completely passive and absolute length measurements can be made for each fiber-sensing gauge. The proposed sensing scheme can be used to measure quasi-distribution strain or temperature. For large-scale smart structures, this technique not only extends the sensors number, but also provides a redundancy for the sensing system. This means that the sensor loop allows one breakdown point, because the sensing system will still be working even if the embedded sensor array breaks somewhere.

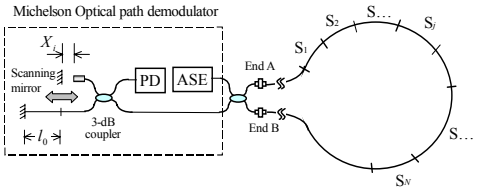

Fig. 1 Schematic of multiplexed fiber optic sensors distributed in single loop.

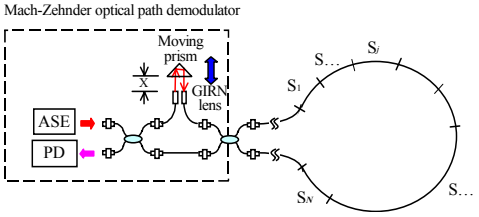

Fig. 2 Schematic of multiplexed fiber optic sensors distributed in single loop.

2.1 Michelson interrogation system

Single loop sensor array using a Michelson interferometer as optical path demodulator is shown in Fig. 1. The light source is an erbium-doped fiber amplifier, which provides up to 10 mW of amplified spontaneous emission (ASE) at the wavelength of 1.55 μm. Low coherence light via a fiber optic isolator is launched into the Sagnac like fiber loop by a fused 3-dB coupler. The fiber loop consists of *N*-section of 1 m length single mode fiber connected in series, forming a loop *N*-sensor array. Reflected light from this fiber loop is coupled into an optical low coherence reflectometer (OLCR). Inside the OLCR, the light signals are split by the second 3-dB coupler. The lower (reference) path is reflected directly by the mirrored fiber end and then leads to photo diode (PD) detector. The upper path leads to the fiber optic collimator and is reflected by a moving scanning mirror, then the signals are guided to PD detector.

The reflectivity of the in-line reflectors between two sensing segments is very small and equal to 1% or less to avoid depletion of the input probe signal. The fiber sensor length l_i between adjacent reflectors can be of any value as long as the differences in their lengths are not larger than the scanning range of the OLCR. In our experiments, l_i is chosen about 1 m long and the reference gauge length l_0 is nearly the same as the sensor length. The length difference between any two of the sensors is within 270 mm corresponding to 400 mm scanning range of the OLCR in free space. As the OLCR is scanned, the white light interference patterns occur whenever the path difference matches the distance between adjacent reflectors in the sensor loop.

2.2 Mach-Zehnder interrogation system

The loop network using a Mach-Zehnder optical path demodulator is shown in Fig. 2. It consists of a light emitting diode (LED) or superluminescent diode (SLD) light source, a PD detector, a fiber optic Mach-Zehnder optical path interrogating part, and a number of fiber segments connected in series, forming a loop network. The light launched into the ring network-sensing array first passes the Mach-Zehnder interrogator and reaches the fiber optic sensor array. The optical path difference (OPD) of Mach-Zehnder interferometer varies with a scanning prism. The scanning prism is used to adjust the OPD of Mach-Zehnder interferometer to match and trace the change of the fiber length in each sensing segment. The OPD of Mach-Zehnder interferometer is made approximately equal to the fiber sensor gauge length, so that two reflected light waves from the surfaces at both ends of each sensing gauge can match each other. When the OPD of Mach-Zehnder interferometer is equal to the gauge length of a particular sensor, a white light fringe pattern is produced. Similar to Michelson interrogator in the central fringe, which is located in the center of the fringe pattern, the highest amplitude peak corresponds to the exact match of the OPD for that sensor. As the optical path of the fiber sensor is modulated by the ambient perturbation, for instance strain or temperature, the perturbation parameters related with the optical path change will be measured and recorded by the shift of the interference signal peak.

2.3 Discussion

For the sensor schemes described above, if the power of light is the same, the intensity of sensor output signal in Mach-Zehnder scheme is larger than that in Michelson scheme. Therefore, if the light source power is lower, Mach-Zehnder scheme is preferred in order to enhance the sensor multiplexing capability. If the power of light source is strong enough, Michelson scheme is preferable because one directional collimator-mirror system is easy in installation and adjustment for the practical system.

3. Principle of operation

The fundamental principle of this bi-direction

optical path interrogation approach is based on optical fiber white light interferometry. As shown in Fig. 3, it consists of two parts linked by a 3-dB coupler: one is the loop sensor array composed of a total number of N fiber optic segments connected each other and the other is Michelson or Mach-Zehnder type optical path interrogator. If the gauge length of the ith fiber optic sensor is l_i in the sensor array loop, the optical signals are reflected from two ends of the fiber optic sensor i. The sensing optical path difference (SOPD) of two reflective optical signals is nl_i, where n is the refractive index of fiber guide mode. The varying compensation path can be adjusted by a scanning mirror (or a prism) mounted on a moving translation stage as shown in Fig. 1 (or Fig. 2 in the case of moving prism). The gauge lengths of sensors (l_1, l_2,…, l_N) are chosen to be slightly different one from another and approximately the same as the sensing optical path-length difference. It can be tuned by the use of scanning mirror or prism system. When the mirror or prism is tuned to a position where the compensation optical path difference (COPD) of the interrogator is matched to the gauge length of a particular sensor, a white light interferometric pattern is generated. The highest amplitude fringe of white light interference pattern located in the center of the fringe pattern corresponds exactly to the matched optical path between SOPD and COPD. If we adjust the variable COPD in Michelson or Mach-Zehnder interrogator to match the SOPD, then by way of tracing and recording the change of COPD $l(X_i)$, the variation of the SOPD can be measured via the measurement of the displacement of the compensation optical path, which corresponds to the change of the fiber optic sensor gauge variation, as shown in Fig. 4. The optical signals reflected from the sensor ends not only come from clockwise direction, as the solid line illustrated in Fig. 3, but also come from counterclockwise direction, as the dotted line shown in Fig. 3, due to the symmetry of fiber loop topology. This is why we call it "bi-direction" interrogating system.

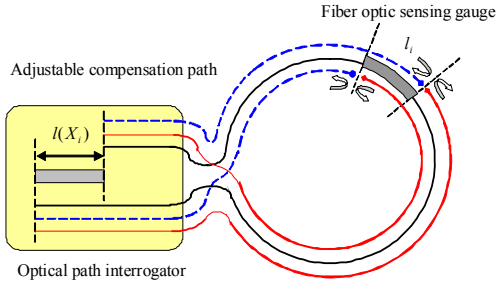

Fig. 3 Working principle of bi-direction optical path interrogator adjusting the compensation path to match each sensor gauge.

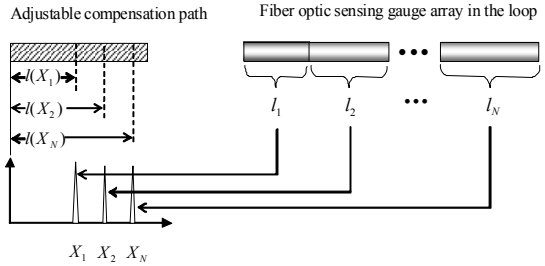

Fig. 4 N unique output optical signals corresponding to each fiber optic sensor gauge in the sensing loop.

Therefore, the deformation of sensor i can be measured by the displacement of the moving mirror:

$$\Delta X_i = \Delta(nl_i)\,. \tag{1}$$

Thus, it can be used as a powerful tool to measure quasi-distribution strain or temperature by the following relationship:

$$\varepsilon_i = \frac{\Delta X_i}{n_{\text{equivalent}} l_i} \tag{2}$$

and

$$(T_i - T_{0i}) = \frac{\Delta X_i}{l_i(T_{0i}) n(\lambda, T_{0i})[\alpha_f + C_T]} \tag{3}$$

where $n_{\text{equivalent}} = n\{1-(1/2)n^2[(1-\nu)p_{12} - \mu p_{11}]$ represents the equivalent refractive index of the fiber guide mode. For silica materials at wavelength $\lambda = 1550$ nm, the parameters are $n = 1.46$, Poisson ratio $\nu = 0.17$, photo-elastic constants $p_{11} = 0.12$, and $p_{12} = 0.27$, taken from [17]. $n(\lambda, T_{0i})$ is the refractive index of the optical fiber under the condition of wavelength λ and the ith sensor ambient temperature T_{0i}. Here, α_f and C_T are the thermal expansion coefficient and the refractive index temperature coefficient of the optical fiber, respectively. $\alpha_T = 5.5\times10^{-7}/\,℃$, $C_T = 0.811\times10^{-5}/\,℃$ at wavelength $\lambda = 1550$ nm

are taken from [18].

4. Multiplexing capacity

With the scanning mirror moving on the translation stage, there will be N groups of interference fringe patterns appear, which correspond to the OPD of the interferometer matched to that of N sensors in the loop. The peak fringe intensity at the photo-detector corresponds to the ith sensor, which is due to the coherent mixing between the reflected waves from the ith and the $(i+1)$th reflectors, and may be expressed as

$$I_D(i)=\frac{I_0}{16}\sqrt{R_f R_m \eta(X_i)}\times \left\{\begin{array}{l}\left[\prod_{k=1}^{i-1}T_k\beta_k\right]\left[\prod_{k=1}^{i-1}T_k'\beta_k'\right]\sqrt{R_i R_{i+1}T_i\beta_i T_i'\beta_i'} \\ \qquad\qquad + \\ \left[\prod_{k=i+2}^{N+1}T_k'\beta_k'\right]\left[\prod_{k=i+2}^{N+1}T_k\beta_k\right]\sqrt{R_i' R_{i+1}' T_{i+1}'\beta_{i+1}' T_{i+1}\beta_{i+1}}\end{array}\right\} \quad (4)$$

where I_0 represents the light intensity coupled into the input optical fiber from ASE source. The insertion loss of the 3-dB coupler has been neglected. β_i and β_i' respectively represent the excess losses associated with sensor S_i, which is due to the connection loss between the sensing segments, for the CW(clockwise) and the CCW(contra clockwise) propagating light waves. T_i (T_i') and R_i (R_i') are respectively the transmission and reflection coefficient of the ith partial reflector. T_i (T_i') is in general smaller than $1-R_i$ ($1-R_i'$) because of the loss factor β_i (β_i'). The values of T_i, R_i, and β_i could be different from that of T_i', R_i', and β_i'. $\eta(X_i)$ is the loss associated with the scanning mirror and collimating optics, and is a function of the scanning mirror position $X_{i,i+1}$, R_f is the reflectivity of the mirrored fiber end and R_m is the reflectivity of the scanning mirror.

In the fiber optic sensors loop array, the fraction of optical source power is coupled into the fiber and distributed over the sensor array via several connectors. Each sensor element absorbs or diverts a certain amount of power (insertion loss), typically between 0.1 dB and 0.5 dB. If the minimum-detecting limit of the photodiode is $I_{\min}$, the maximum number of total fiber optic sensors which can be evaluated are those sensors satisfying the condition of

$$I_D(i)\geq I_{\min}. \quad (5)$$

In calculation, the excess insertion loss of two 3-dB couplers is neglected and the typically fiber optic connection insertion loss coefficients β_i and β_i' are assumed to be 0.9 (i = 0, 1, 2,…, N). Under the condition of perpendicular incidence, the reflectivity at the fiber end surface is given by Fresnel formula $R=(n-1)^2/(n+1)^2$, where n is the index of the fiber core, and the typical value is 1.46, corresponding to 4 percent reflectivity. For good butt-connected fiber ends, the air gap is smaller then one wavelength, in that case the typically reflectivity R_i ($=R_i'$) is close to 1%. Therefore, the transmission coefficient can be calculated as $T_i=T_i'=0.89$. We assume that the average attenuation of the moving mirror part is 6 dB, i.e. $\eta(X_i)=1/4$. Then, the normalized optical signal intensity vs. the fiber optic sensor number i is plotted in Fig. 5(a) for different sizes sensor loop array. In comparison with the open loop case, the sensor multiplexing capability is extended as much as twice, as shown in Fig. 5(b).

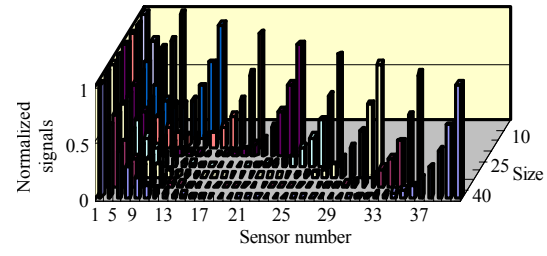

(a)

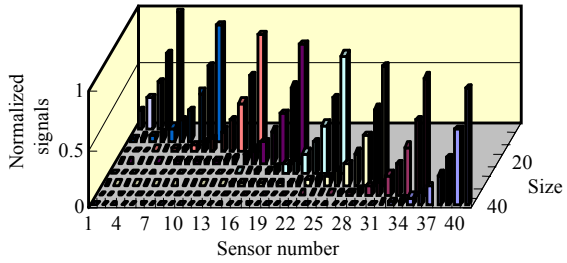

(b)

Fig. 5 Normalized output signal intensities for different fiber sensor loop sizes: (a) loop closed and (b) loop opened.

5. Performance of the sensing system

If two or more break points occur in the fiber sensor loop, the sensors between two broken points will fail. This is different from the case of only one break point occured in the fiber loop. In general, if just one point is broken in the fiber loop, the intensity of each sensor's output signal will be decreased because the output signal in each sensor is only supplied by one of two branches. When the light power is lower than the minimum requirement, the signals of the sensors far from the interrogator ports will be emerged in the noise floor. The extreme case is that the break point is closed to port A or port B (see Fig. 1).

Figures 1 and 2 show the experimental arrangement used to demonstrate the looped fiber optic white light interferometric sensor array. An ASE light source is used in our experiment. The unpolarized light power of the ASE source is adjustable in the range of 0 – 10 mW. Ten optical fiber segments are connected each other and used as fiber optic sensors. The fiber optic sensor gauge length is chosen nearly 1 m. The difference of each sensor gauge length is about 7 mm and connected each other by butt-connectors. The output signal intensity of the 10-sensor array are given in Fig. 6 for both loop-closed and loop-open at end A (see Fig. 1).

It can be seen that the results shown in Figs. 6(a) and 6(b) essentially provide the same measurement information in terms of the positions of the peaks. This means that the system will function the same even if one end of the loop is opened. However, the signal level for the loop-closed case is higher than the loop-opened case.

For the used light level of 0.47 dBm, the signal level of sensor S_1 is obviously small in the peak position when the loop is open at end A (Fig. 6 (b)). The same will be true for the sensors near port B if it is open at end B (see Fig. 1) due to the symmetry of the loop architecture. The signal level is significantly enhanced when the loop is closed (Fig. 6(a)). This means that, for the same source power level, the maximum number of sensors can be increased for the closed loop configuration.

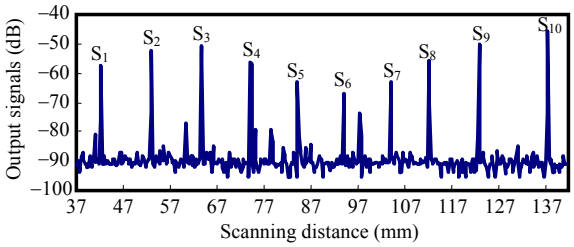

(a)

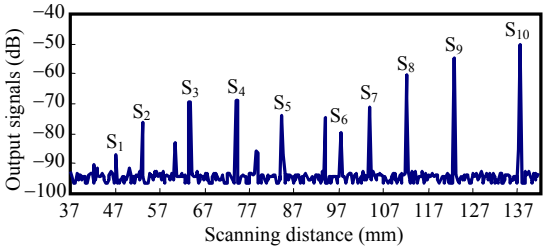

(b)

Fig. 6 Output from the ten-fiber optic sensor array with input light source power of 0.47 dBm.

An important requirement for a fiber optic sensor system is its redundancy ability, especially if the sensor chain is embedded into the structure. In order to test the redundancy performance of the bi-direction interrogation fiber optic sensing system, the fiber optic loop disconnected experiment has been made in both cases of looped fiber sensor chain and the sensors linked in a linear array along a fiber line. The test results are plotted in Fig. 7. We have disconnected the sensor chain between 7th and 8th sensors for the all ten-sensor chain. It can be seen that the output signals of the sensors 1–7 are vanished in the case of ten-sensor array in one fiber line and interrogating from one port, as shown in Fig. 7(b). However, ten sensors are still working when disconnected between 7th and 8th sensors. The output signals, as shown in Fig. 7 (a), are still there except that the signal amplitude near the 8th sensor becomes lower.

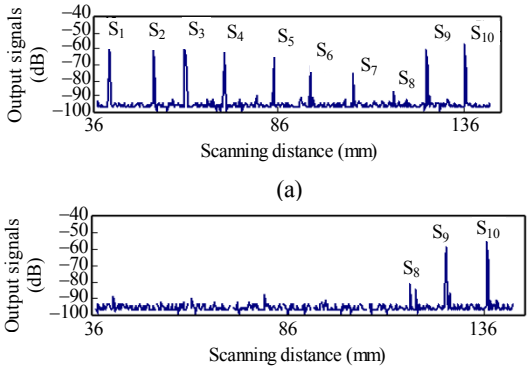

Fig. 7 Redundancy of bi-direction interrogating fiber optic sensor loop topology: (a) output signals in the case of loop open between 7th and 8th fiber optic sensors and (b) output signals in the case of fiber optic sensor array open between 7th and 8th sensors.

It should be mentioned that, although the measurement results of a linear array with loop open at either end A or B are polarization independent (in the strict sense, the effect of polarization is neglected in that case), the results obtained from the closed loop measurement are under the influence of polarization states. Figure 8 shows the variation of the signals when the polarization controller in the loop (see Fig. 1) is adjusted. This is because light signals that are not reflected at the partial reflectors (transmitted) will mix coherently at the loop coupler as they travel through the optical path length. When the counter-propagating (transmitted) light signals are of the same polarization state, the light signal at the output port of the loop will approach zero due to destructive interference [19]. When the counter-propagating signals are of different polarizations, the orthogonal polarization components will add up in intensity and result in a noise floor. The variation of deformation in each gauge length of the sensor starting from the first sensor will change the state of polarization. In that case, their multi-sensing capability will have been reduced. It may therefore be necessary to control the polarization states in order to achieve the optimal results. One method is to insert a de-polarizer between ASE light source and 3-dB coupler, the other solution is to use polarization maintaining fiber in the sensing system to overcome the unstability of polarization state.

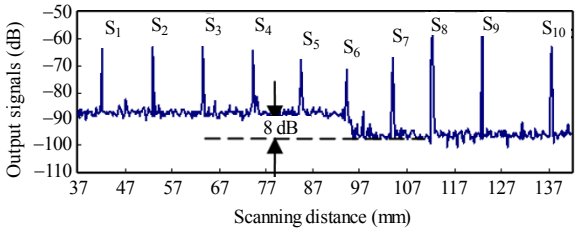

Fig. 8 On the condition of input light source power is 0.47 dBm, a 8-dB reduction in the noise floor is achieved by adjusting the polarization states.

5. Conclusions

The telecommunication industry has long known the advantages of using optical fiber to send information over great distances. Now the security industry is exploring to use the same technology for intrusion monitoring of long perimeter. By using white light interferometric technology, a multiplexed fiber optic deformation sensor based on loop topology network which is suitable for perimeter security applications has been designed and demonstrated in this paper. The sensor system is based on white light Michelson or Mach-Zehnder interferometer as optical path demodulator. Such a loop topology is useful to construct sensor network for distributed sensing. From the view of scanning range of the translation stage, the multiplexing system permits to demodulate over 50 fiber sensors. This kind of fiber optic perimeter monitoring technology could provide cost-effective, high performance, and distributed sensing solutions for the critical infrastructures, high-value military, and civilian sites. These systems are capable of detecting and locating the point of intrusion along the fiber sensing line. However, it is clear that the multiplexed sensors in the single loop network suffer from relatively large fiber segments-induced optical reflective and excess insertion losses that generally limit the total number of sensors which can be accommodated in this configuration.

Acknowledgment

This work was supported by the key project of Nature Science Foundation of Heilongjiang Province (No. ZD200810) and Key Project Foster Program for University and College Science and Technology Innovation (No. 708030), and partially supported by the National Nature Science Foundation of China, under grant number 60877046, 60707013, and 60807032, to the Harbin Engineering University.

References

[1] J. P. Dakin, J. Pearce, and P. Strong, "A novel distributed optical fiber sensing system enabling location of disturbances in a Sagnac loop interferometer," in *Proc. SPIE* , vol. 838, pp. 325, 1987.

[2] S. J. Spammer, P. L. Swart, and A. Chtcherbakov, "Merged Sagnac-Michelson interferometer for distributed disturbance detection," *Journal of Lightwave Technology*, vol. 15, no. 6, pp. 972–976, 1997.

[3] M. Szustakowski, W. Ciurapiński, M. Życzkowski, and N. Pałka, "Recent development of fiber optic sensors for perimeter security," in *35th Annual 2001 International Carnahan Conference on Security Technology*, London, October 16–19, pp. 142–148, 2001.

[4] D. Donlagić and B. Culshaw, "A forward propagation fully distributed microbend sensor system," in *International Conference on Optical Fiber Sensors*, Venice, October 11–13, pp. 662–665, 2000.

[5] Qizhen Sun, Deming Liu, Hairong Liu, Yi He, and Junguo Yuan, "Distributed disturbance sensor based on a novel Mach-Zehnder interferometer with a fiber-loop," in *Proc. SPIE*, vol. 6344, pp. 63440k, 2006.

[6] Tian Lan, Chunxi Zhang, Lijing Li, Guangming Luo, and Chen Li, "Perimeter security system based on fiber optic disturbance sensor," in *Proc. SPIE*, vol. 6830, pp. 68300J, 2007.

[7] A. D. Kersey and W. W. Morey, "Multiplexed Brag grating fiber-laser strain-sensor system," *Electronics Letters*, vol. 29, no. 1, pp. 112–114, 1993.

[8] G. Duck and M. M. Ohn, "Distributed Bragg grating sensing with a direct group-delay measurement technique," *Optics Letters*, vol. 25, no. 2, pp. 90–92, 2000.

[9] E. Sensfelder, J. Burck, and H. J. Ache, "Characterization of a measurement of leakages in tanks and pipelines," *Applied Spectroscopy*, vol. 52, no. 10, pp. 1283–1298, 1998.

[10] T. Horiguchi, K. Shimizu, T. Kurashima, M. Tateda, and Y. Koyamada, "Development of a distributed sensing technique using Brillouin scattering," *Journal of Lightwave Technology,* vol. 13, no. 7, pp. 1296–1302, 1995.

[11] S. A. Al-Chalabi, B. Culshaw, and D. E. N. Davies, "Partially coherent sources in interferometry," in *Proceedings of 1st International Conference on Optical Fiber Sensors*, London, April 26–28, pp. 132−135, 1983.

[12] J. L. Brooks, R. H. Wentworth, R. C. Youngquist, M. Tur, B. Y. Kim, and H. J. Shaw, "Coherence multiplexing of fiber optic interferometric sensors," *Journal of Lightwave Technology*, vol. LT-3, no. 5, pp. 1062–1072, 1985.

[13] V. Gusmeroli, "High-performance serial array of coherence multiplexed interferometric fiber-optic sensors," *Journal of Lightwave Technology*, vol. 11, no. 10, pp. 1681–1686, 1993.

[14] W. V. Sorin and D. M. Baney, "Multiplexing sensing using optical low-coherence reflectometry," *IEEE Photonics Technology Letters*, vol. 7, no. 8, pp. 917–919, 1995.

[15] D. Inaudi, S. Vurpillot, and S. Lloret, "In-line coherence multiplexing of displacement sensors, a fiber optic extensometer," in *Proc. SPIE*, vol. 2718, pp. 251–257, 1996.

[16] Libo Yuan, Limin Zhou, Wei Jin, and Jun Yang, "Low-coherence fiber-optic sensor ring network based on a Mach-Zehnder interrogator," *Optics Letters*, vol. 27, no. 11, pp. 894–896, 2002.

[17] Libo Yuan, Wei Jin, Limin Zhou, Y. H. Hoo, and S. M. Demokan, "Enhanced multiplexing capacity of low-coherence reflectometric sensors with a loop topology," *IEEE Photonics Technology Letters*, vol. 14, no. 8, pp. 1157–1159, 2002.

[18] C. D. Butter and G. B. Hocker, "Fiber optic strain gauge," *Applied Optics*, vol. 17, no. 18, pp. 2867–2869, 1978.

[19] L. B. Yuan, "Optical path automatic compensation low-coherence interferometric fiber optic temperature sensor," *Optics & Laser Technology*, vol. 30, no. 1, pp. 33–38, 1998.